



MINISTRY OF TECHNOLOGY

AERONAUTICAL RESEARCH COUNCIL

CURRENT PAPERS

Leading Edge Effects on
Caret Wings

by

J. C. Cooke

LONDON: HER MAJESTY'S STATIONERY OFFICE

1968

PRICE 4s 6d NET

LEADING EDGE EFFECTS ON CARET WINGS

by

J. C. Cooke

SUMMARY

The two planes of the lower surface of a caret wing are treated as though they were infinite and swept, and the leading edge shock boundary layer interaction for each is investigated. It is found that the shock shapes are curved near to the leading edge and the pressure there is higher than the design pressure. However, in certain circumstances each shock may soon become parallel to the design shock and the pressure near to its design value. In extreme conditions this may never happen and for these cases it is concluded that the design is not achieved. A tentative condition for the achievement of design conditions is given.

CONTENTS

	<u>Page</u>
1 INTRODUCTION	3
2 WEAK INTERACTION	4
3 STRONG INTERACTION	5
4 THE SHOCK SHAPE	5
5 EXAMPLES	6
6 RESULTS AND DISCUSSION	7
7 A CRITERION FOR CARET FLOW	8
8 CONCLUSIONS	10
SYMBOLS	11
REFERENCES	12
APPENDIX 1 - Streamwise slope of the shock	13 - 15
ILLUSTRATIONS - Figs.1 to 7	-
DETACHABLE ABSTRACT CARDS	-

ILLUSTRATIONS

	<u>Fig.</u>
The caret surface	1
Probable actual situation	2
Projection on a sphere, centre the apex	3
Pressure ratio, case 1	4(a)
Pressure ratio, case 2	4(b)
Shock position and pressure distribution at the trailing edge	5
Co-ordinate system for Appendix 1	6
Projection on a sphere centre the point O where the incident ray meets the shock	7

1 INTRODUCTION

Caret or Nonweiler¹ wings have the property that there is an attached plane shock at the base (see Fig.1), supposing the leading edges to be sharp; after passing through the shock the air flow is everywhere parallel to the ridge line. The leading edge may, however, not be sharp and in any case the growth of the boundary layer is such that the displacement surface is rounded. Consequently, the shock in fact stands off from the surface, but it may still be plane over most of the region of interest, in which case it may appear as in Fig.2, and the basic mechanism of the design will still work. This, indeed has so far been found to be the case in experiments, which have mostly been at sufficiently low Mach numbers and high Reynolds numbers for the effect to be confined to such a small region near to the leading edge as scarcely to be seen. The effect is known to depend on the parameter χ equal to $M^2/R_x^{1/2}$, the boundary layer interaction parameter. In the literature the effect has been divided into two parts, the so-called "strong" interaction which occurs near to the leading edge and the "weak" interaction which occurs a little further downstream. These are asymptotic states characterized by $K \gg 1$ and $K \ll 1$ where $K = M\theta$, in which θ is the angle of turning through the shock. Nearer still to the leading edge there may be a region of flow with "slip" and nearer still a "free-molecule" regime. We shall only consider here the weak and strong interaction regimes, and indeed mainly only the weak interaction case. We shall suppose the flow to be laminar throughout.

The simple caret wing has two plane surfaces underneath and, for simplicity, in order to gain some idea of the effect, we shall suppose each of these planes to be extended so as to be semi-infinite, their leading edges being straight extensions of that of the caret; these plates may have rounded leading edges. We shall only consider their lower surfaces. These plane surfaces cannot of course really act independently of each other, but we may expect the leading edge effects to be independent if we are not too close to the apex, which is excluded altogether from the analysis. We shall find that the shocks at the edges are in fact curved, as in Fig.2, but that near the middle they may become parallel and it seems reasonable to suppose that they join up. On the other hand there may be cases in which they never become parallel, and so there must in such a case be an interaction between the surfaces, the nature of which it is not possible to determine at present. A better model might be to treat the flow as conical (instead of cylindrical) but this renders the analysis difficult or impossible to carry out at present.

So far in weak interactions it has only been possible to carry out the analysis in two dimensions and for either the boundary layer displacement effect on infinitely thin flat plates, or the thickness effect without the displacement effect. It has not been possible to combine the two effects, though it has been shown that, as far as pressures are concerned, fair agreement with experiment can be obtained simply by adding the pressures for the two cases independently²; this has been done in the present work. Once the pressure is known it is possible to work out the shape of the shock. For strong interactions Cheng, Hall, Golian and Hertzberg³ have been able to combine the two effects and obtain what they call a zero-order approximation in $(\gamma - 1)/(\gamma + 1)$. For the cases we are considering here, which are highly swept, the method is not applicable, since in our case the strong shock region is too near to the rounded nose for the theory to apply.

2 WEAK INTERACTION

If the leading edge is sharp and unswept but at an incidence α , the growth of pressure is given by⁴

$$\frac{p}{p_\alpha} = 1 + \frac{b_\alpha M_\alpha^3}{R_\alpha x^2} \quad (1)$$

where the suffix α refers to inviscid sharp wedge conditions at incidence α , that is, conditions behind the straight shock at the leading edge. In this equation b_α is given by

$$b_\alpha = \gamma \left[\frac{0.865 T_w}{M_\alpha^2 T_\alpha} + 0.166 (\gamma - 1) \right] \quad (2)$$

where T_w is the wall temperature, assumed constant.

If the plate is now swept, the boundary layer growth should proceed in approximately the same way and equation (1) should still apply provided x is measured along the section of the plate by a vertical plane containing the direction of the oncoming flow. We should note that the independence principle does not apply in these high supersonic flows.

If the plate is unswept and the leading edge is blunt with diameter or thickness d the pressure due to this is given by

$$\frac{p}{p_\alpha} = 1 + \frac{p_\infty}{p_\alpha} \frac{Bc M_\infty^2}{(x/d)^{2/3}} \quad (3)$$

where $B = (\frac{1}{2})^{2/3}$, $c = c_\gamma (C_D)^{2/3}$, C_D being the drag coefficient of the leading edge for flow normal to its and $c_\gamma = 0.112$ for air and 0.169 for helium.

If the plate is now swept, equation (3) still applies, provided C_D is replaced by $C_D \cos^2 \phi$, where ϕ is the angle of sweep. One must be careful here about the definition of ϕ ; actually, its value is to be taken as $(90^\circ - \text{the angle between the incident direction of flow and the leading edge})$. Creager⁴ gives this factor as $\cos^3 \phi$, but it can be shown that he is in error here. (Indeed his experiments suggest that the power 3 is far too large and ought to be replaced by 1, not 2 as given here on theoretical grounds.)

Finally, the combination of displacement and thickness effects are added. There is no theoretical justification for this, but apparently it gives results in agreement with experiment⁴. Hence the pressure ratio p/p_∞ can be found, the full formula being

$$\frac{p}{p_\infty} = \frac{p_a}{p_\infty} \left\{ 1 + b_\alpha \frac{M_\alpha^3}{R_{\alpha x}^2} \right\} + \frac{Bo M_\infty^2}{(x/d)^{2/3}} \quad (4)$$

where b_α is given by (2), $B = (\frac{1}{2})^{2/3}$, $\alpha = c_Y (C_D \cos^2 \phi)^{2/3}$, $c_Y = 0.112$ for air.

3 STRONG INTERACTION

It can be shown that the approximate analysis of Cheng et al.³ still applies to a swept flat plate at incidence. We measure everything streamwise and the only difference is in the drag coefficient of the leading blunt edge. If the unswept drag coefficient is C_D (denoted by k by Cheng et al.) we simply write $C_D \cos^2 \phi$ in place of C_D , as indeed we did in section 2. Then all the analysis will still apply and in particular we can find from their curves the value of the pressure ratio. We have recomputed these curves so as to be able to plot them on a larger scale and to extend their range.

In the work of Cheng et al. it is necessary for $M_\infty \delta$ to be large, whilst δ should be small. In many cases there can be found a range of values of δ between which both these relations hold sufficiently well for the analysis to be valid. Cheng et al. give a pair of inequalities which determine this range. It is found for the examples considered here that there are no values of δ which satisfy both these inequalities simultaneously, and so we shall give no further details here.

We have nevertheless described the modification to the analysis of Cheng et al. which is required to take sweep into account, since it is simple and may well be applicable if models of less sweep are ever contemplated.

4 THE SHOCK SHAPE

If the position of the shock at some point near to the leading edge is known, and its streamwise slope is known at all points downstream the position of the shock can be obtained by integration. For simplicity of description we shall take the incident flow as horizontal, and then we take as "base plane" a horizontal plane through P, the point of the leading edge under consideration. Distance X is measured from P in this plane downstream and Y is measured perpendicular to this plane. We must therefore find the streamwise slope of the shock at points downstream of P, knowing the pressure rise p/p_∞ across it. This is a problem of three dimensional geometry, together with the shock relations across an oblique shock and is discussed in Appendix 1. Provided that ζ is small where ζ is the angle between the free stream and the tangent plane to the shock, it can be shown that the streamwise slope of the shock is approximately $\tan \zeta$ and so, if Y_s is the Y co-ordinate of the shock, we have

$$Y_s = \int_{X_0}^X \tan \zeta \, dX + Y_0 \quad (5)$$

where (X_0, Y_0) are to co-ordinates of the starting point. Now ζ is found from the shock relation

$$\frac{p}{p_\infty} = \frac{7M_\infty^2 \sin^2 \zeta - 1}{6} \quad (6)$$

and so we can find the position of the shock.

Near to the leading edge it may be necessary to use the more accurate formula of Appendix 1. In this region the direction of flow after the shock is no longer streamwise so the basic flow is not so nearly achieved. Consequently, the greater apparent accuracy of the full formula may not have much justification.

5 EXAMPLES

We shall consider two cases for which boundary layer calculations were made by Catherall⁵, the details being as shown below:-

TABLE 1

Case	Height	ζ_c	δ_c	M_∞	T_w	R_{ax}	d/c	T_∞	M_α
1	200,000 ft	10.1	4.1°	8	600°K	3.003×10^6	0.005	254°K	7.065
2	300,000 ft	7.046°	1.046°	9	600°K	3.68×10^6	0.005	197°K	8.692

Each of these has a chord of 200 feet and so we are taking in each case a leading edge diameter d of 1 foot. Each has a ridge angle of 6° and the angle ξ is 66.7° . (See Fig.3.) The other angles concerned may best be calculated from spherical trigonometry and their values are shown in Fig.3 which represents the projection of the body on a sphere whose centre is the apex. The particular features of these are that in case 1 the displacement thickness is very small, and so is its slope over most of the body. In case 2 the displacement thickness is very much larger owing to the much lower Reynolds number, and it seems possible that for this case the leading edge effect might not be confined to a very small region of the body. We have assumed that the wall is cooled sufficiently for its temperature T_w to be constantly equal to 600°K in each case.

We use equation (4) to calculate the pressure ratio at various points downstream of the leading edge. This equation reduces to

$$\frac{p}{p_\infty} = a' + b' \left(\frac{x}{c} \right)^{-1/2} + c' \left(\frac{x}{c} \right)^{-2/3} \quad (7)$$

where the constants a' , b' and c' are given by

TABLE 2

	a'	b'	c'
Case 1	2.13	0.0507	0.0404
Case 2	1.42	0.593	0.0468

The values of a' are in fact the amount of pressure rise if there were no interaction effect. The term in b' represents the displacement effect and that in c' the thickness effect. We have taken $C_D = 2$ as a reasonable value, suggested by Cheng et al.⁴. It of course varies with the shape of the leading edge.

The results for pressure rise are given in Fig.4. Note that the scale of x/c has been stretched near to the leading edge by plotting $(x/c)^{\frac{1}{2}}$ as abscissa. As the leading edge is approached the pressure ratio rises and indeed tends to infinity as x/c tends to zero. This cannot happen really and the error is due to the fact that the analysis is being extended to the region of the bow shock where it does not apply. However it is possible to calculate the maximum value that the pressure rise through the shock can have. The tangent plane to the shock is swept and the maximum possible value of the normal component is $M_\infty \cos \phi$. From this the pressure rise can be calculated. We have therefore extrapolated the pressure curves to this value and adopted the resulting relation as a means of calculating the shock position, provided that this position is known at some point. We do not know this as it depends on the stand-off distance of the shock. What we have done is started from a point not too near to the leading edge and adjusted the value of Y there so that the resulting curve passes smoothly through the leading edge. Actually it will stand off a small distance further than this, but inaccuracies here scarcely affect the overall picture.

Finally we have plotted the calculated positions of the two shocks at the trailing edges for each of the two cases in Fig.5. It must be realised that the shock is not conical in this figure. If we wish to find the shock position at say half way down the body we must cut off the figure by two vertical lines half way out as shown dotted in the figure and exclude the middle part, moving the two outside parts towards each other until they meet.

6 RESULTS AND DISCUSSION

It will be seen that for case 1 the shocks are compatible over a large part of the body. They are curved at the edges, but one may well expect that the design flow will in fact be achieved and design shock will be present, though slightly displaced from its design position. The two sides will not interact except very near to the apex.

On the other hand, we see that in case 2 the shocks are not compatible anywhere and the two sides must interact everywhere. It is possible that the flow adjusts itself in such a way that there is one uniform rounded shock, but at any rate it seems certain that the basic feature of the caret wing is not at all closely achieved. There is a sideways pressure gradient everywhere inside the wing which will make the surface flow curve inwards, so that the flow pattern on which the calculation was based does not apply. This is in contrast to case 1 where the pressure is constant over a large part of the surface. (It should be remembered that in Fig.4 the part near to the leading edge has been stretched by the method of plotting. The pressures are correctly scaled in Fig.5.)

7 A CRITERION FOR CARET FLOW

On the basis of this work we suggest a highly tentative criterion for the existence of the planned caret flow. The basic interaction parameter χ_α is given by

$$\chi_\alpha = \frac{M_\alpha^3 C_\alpha^{\frac{1}{2}}}{R_{\alpha x}^{\frac{1}{2}}}$$

The constant C_α comes from the Chapman Rubesin formula. χ_α is what was called χ_{orig} by Hayes and Probstein⁶. It is generally taken that the effect of the interaction is negligible in regions where the parameter χ_α has a value less than unity. We will suppose that if the effect only takes place in a region 5% of the total chord from the leading edge the basic caret wing theory will work reasonably well in practice. We give below the values of χ_α for the two examples at various values of x/c . It will be sufficient here to take $C_\alpha = 1$.

TABLE 3

Case 1		Case 2
x/c	χ_α	χ_α
0.05	0.77	14.5
0.1	0.54	10.3
0.2	0.38	7.3
0.4	0.27	5.0
0.8	0.19	3.6
1.0	0.17	3.2

Thus we see that for case 1 the criterion $\chi_\alpha < 1$ is satisfied at 5% chord from the leading edge, whilst for case 2 it is nowhere satisfied. A glance at Fig.5 suggests that we are being somewhat conservative in our choice of unity for the maximum value of χ_α , and that possibly a larger value might be used.

For convenience it may be preferable to give the maximum allowable value of χ_α based on the full chord. We denote this by $\chi_{\alpha c}$. The result is

$$\chi_{\alpha c} = \frac{M_\alpha^3}{R_{\alpha c}^{\frac{1}{2}}} = 0.22 \quad (8)$$

For values greater than this one may have doubts as to whether the design caret flow will be achieved.

One of the experiments of Sykes⁸ was made at a Mach number of 10.3, with a design value of $\zeta_D - \delta_D$ equal to 5° . There are two possible configurations satisfying the design conditions for this model, one with $\zeta_D = 8^\circ$, $\delta_D = 3^\circ$ and the other with $\zeta_D = 20^\circ$, $\delta_D = 15^\circ$. The Reynolds number of the tests was 1.4×10^5 per inch and there were two models, one with a sweep of 50° and length 4.3" and the other with a sweep of 70° and length 9.9".

For these models the results are:-

δ_D	ϕ	$\chi_{\alpha c}$
3°	50°	0.82
	70°	0.54
15°	50°	0.18
	70°	0.12

It will be seen that the maximum value of $\chi_{\alpha c}$ is exceeded for both sweep angles for the weak shock case, that is when $\delta_D = 3^\circ$, particularly for the model with the least sweep. The experiments do in fact show some divergence from design for this incidence, and it is larger for the lower sweep angle. On the other hand, for $\delta_D = 15^\circ$, $\chi_{\alpha c}$ is below the criterion given here, and indeed design conditions were well fulfilled for this case. It may be possible that the value 0.22 in equation (8) could be raised a little without prejudicing the design too much.

We may note that for the caret wing tested by Squire⁷ (his model 2) the value of $\chi_{\alpha c}$ was only 0.01.

Leading edge thickness has some effect on the results; we have taken a fairly large value for this in our numerical examples. If it were thinner the effect would be reduced although the value of $\chi_{\alpha c}$ is not changed. Hence for a thinner leading edge it may be possible to use a larger value of $\chi_{\alpha c}$ than the one suggested. It will be noticed, however, that the thickness effect does not depend on Reynolds number. Consequently for the lower Reynolds numbers, as in case 2, the thickness effect is almost entirely masked by the larger displacement effect as can be seen from equation (7) and Table 2, and quite large changes in thickness may be made without affecting the overall picture very much.

8 CONCLUSIONS

The analysis of this paper shows that if the interaction parameter $\chi_{\alpha c} = M_{\alpha}^3 / R_{\alpha c}^{\frac{1}{2}}$ is large enough the flow aimed at in the design of caret wings may not be achieved. If each side is calculated independently the shapes of the shocks may be found approximately in places not too near to the leading edges. The two shocks thus obtained may meet at an angle and cannot join up, so that there must be some interaction between the two sides. What happens in such a case cannot be determined by the simple methods adopted here, and the whole flow must be considered afresh.

However, for smaller values of χ , the two sides may well be considered to be independent of one another, and the two shocks merge properly, except for a small region near to the apex. In this case the design is probably achieved except near to the leading edges.

An attempt has been made to estimate the conditions for which the design flow may occur. If M_{α} is the caret design Mach number after the shock is passed and $R_{\alpha c}$ the corresponding Reynolds number based on the maximum chord, a tentative value for achieving design flow is

$$\chi_{\alpha c} = \frac{M_{\alpha}^3}{R_{\alpha c}^{\frac{1}{2}}} \leq 0.22$$

and design flow may not be achieved if this value is exceeded.

In most of the tests so far made $\chi_{\alpha c}$ has been well below the maximum value suggested. In order to estimate the value of such a criterion it will be necessary for tests to be made at higher values of $\chi_{\alpha c}$. This may be difficult, but it seems essential if one is considering flight at very high altitudes such as that suggested in case 2 of this paper, which fits into the suggested corridor⁵ for flight at great heights and large Mach numbers.

The value of $\chi_{\alpha c}$ may well be an important consideration in deciding the characteristics of any future wind tunnel which may be built to investigate flight at large altitudes and hypersonic speeds.

SYMBOLS

a', b', c'	constants in (7)
b_α	given by (2)
B	$(1/2)^{2/3}$
c	$c_\gamma (C_D)^{2/3}$ in equations (3) and (4)
c	maximum chord
C	constant in relation $\mu/\mu_1 = C(T/T_1)$
c_γ	constant (0.112 for air, 0.169 for helium)
C_D	drag coefficient of the nose
d	diameter or width of the nose
M	Mach number
p	pressure
R_x	Reynolds number based on distance x
T	temperature
x	streamwise distance along the surface
X	streamwise distance along the base plane
Y	distance from base plane
Z	distance normal to the XY plane
γ	specific heat ratio
ϵ	$\tan \zeta_D - \tan \zeta$
δ	turning angle through shock
ζ	angle between tangent plane to shock and incident direction of flow
μ	coefficient of viscosity
ξ	angle between planes of caret and vertical plane
ϕ	angle of sweep
χ	$M^3/R^{\frac{1}{2}}$

SYMBOLS (CONTD)

Subscripts

∞	refers to conditions at infinity upstream
α	refers to conditions in inviscid flow after passing through the shock
D	refers to caret design condition
c	refers to quantities based on the centre-line chord c
w	refers to conditions on the wall

REFERENCES

<u>No.</u>	<u>Author</u>	<u>Title, etc.</u>
1	Nonweiler, T.R.F.	Delta wings of shapes amenable to exact shock-wave theory. A.R.C. 22,644, 1961
2	Creager, M.O.	Effects of leading-edge blunting on the local heat transfer and pressure distributions over flat plates in supersonic flow. NACA TN No.4142, 1957
3	Cheng, H.K. Hall, J.G. Golian, T.C. Hertzberg, A.	Boundary-layer displacement and leading-edge bluntness effects in high-temperature hypersonic flow. J. Aero Sci., Vol.28, p.353, 1961
4	Creager, M.O.	The effect of leading-edge sweep and surface inclination on the hypersonic flow field over a blunt flat plate. NASA Memo 12-26-58A, 1959
5	Catherall, D.	Boundary layer characteristics of caret wings. A.R.C. C.P.694, May 1963
6	Hayes, W.D. Probstein, R.F.	Hypersonic flow theory. Academic Press, New York and London, 1959
7	Squire, L.C.	Pressure distributions and flow patterns at $M = 4.0$ on some delta wings of inverted 'V' cross section. R.A.E. T.N. No. Aero 2838, A.R.C. R&M 3373 August 1962
8	Sykes, D.M.	Flow visualisation studies of plane and caret delta wings at supersonic and hypersonic Mach numbers. R.A.R.D.E. Memo (B) 59/62. 1962 A.R.C. 24,393

APPENDIX 1

STREAMWISE SLOPE OF THE SHOCK

Assume for convenience of description that the incident flow is horizontal and in the direction of the X axis, that OY is vertically downwards, and OZ is normal to OX, where O is the point where the incident ray under consideration would reach the design shock of the caret. (See Fig.6.)

Then the equation of the design shock is $Y = X \tan \zeta_D$. This shock contains the leading edge, which makes an angle $90^\circ - \phi$ with OX. Hence the equation of the leading edge (expressed with the denominators as actual direction cosines) are

$$\frac{X - a}{\sin \phi} = \frac{Y - b}{\sin \phi \tan \zeta_D} = \frac{Z - c}{(1 - \sin^2 \phi - \sin^2 \phi \tan^2 \zeta_D)^{\frac{1}{2}}}$$

where (a, b, c) are the co-ordinates of some point on the leading edge.

Now let

$$\cos \alpha = \tan \phi \tan \zeta_D$$

and the leading edge becomes

$$\frac{X - a}{\sin \phi} = \frac{Y - b}{\cos \alpha \cos \phi} = \frac{Z - c}{\sin \alpha \cos \phi} .$$

We now suppose that in fact the incident flow hits an oblique shock, the equation of whose tangent plane at the point of impact is

$$\ell X + mY + nZ = D ,$$

where $\ell^2 + m^2 + n^2 = 1$, so that ℓ , m and n are the actual direction cosines of its normal. Now the incident flow makes an angle ζ with its projection on the plane of the shock, that is, $90^\circ - \zeta$ with the normal to the shock. Hence we have $\ell = \sin \zeta$.

Again, in this infinite swept model, the leading edge must be parallel to the tangent plane to the shock, that is, perpendicular to the normal to the shock. Hence

$$\ell \sin \phi + m \cos \alpha \cos \phi + n \sin \alpha \cos \phi = 0 . \quad (9)$$

Now

$$m^2 + n^2 = 1 - \ell^2 = \cos^2 \zeta .$$

Hence

$$m = -\cos \zeta \cos \beta, \quad n = -\cos \zeta \sin \beta ,$$

where β is angle to be determined. Equation (9) becomes

$$\sin \zeta \sin \phi - \cos \alpha \cos \beta \cos \phi \cos \zeta - \sin \alpha \sin \beta \cos \phi \cos \zeta = 0 ,$$

that is

$$\tan \zeta \tan \phi = \cos(\alpha - \beta) ,$$

and so β can be found.

The section of the tangent plane to the shock by the plane $Z = 0$ is

$$\ell X + mY = D ,$$

and so the streamwise slope of the shock is equal to

$$\begin{aligned} -\frac{\ell}{m} &= \frac{\sin \zeta}{\cos \beta \cos \zeta} = \frac{\tan \zeta}{\cos[\alpha - (\alpha - \beta)]} \\ &= \frac{\tan \delta}{\cos \{ \cos^{-1}(\tan \zeta_D \tan \phi) - \cos^{-1}(\tan \zeta \tan \phi) \}} . \quad (10) \end{aligned}$$

This result can also be obtained by spherical trigonometry, and to some this may be a preferable way of finding it, since by projecting the figure on a sphere it is possible to see some of the directions of flow involved, particularly that of the emergent ray.

We consider some point O on the shock, and take it as the centre of a sphere (See Fig.7). Through O we draw (1) a line OA parallel to the leading edge, (2) a plane OIZ parallel to the "base plane", and (3) a plane $ONAZ$ parallel to the design shock of the caret. These are projected on to the sphere. The tangent plane to the actual shock, which passes through the line OA (for an infinite swept plate) is also drawn. This produces the great circle AN' . The incident direction of flow is OI , and $IOA = 90^\circ - \phi$ from the definition of sweep. Now the plane containing the incoming and outgoing directions of flow is perpendicular to the shock and so is represented by the line IN' , of "length" ζ , the angle between the incident ray and the shock. The ray will emerge in the direction OS' , where $IS' = \delta$, the turning angle, which may be calculated from the shock relations, if ζ is known. From the figure we see that the streamwise slope of the shock must be $\tan IQ$. If the design flow were achieved the incident ray OI would emerge along OS , with $IN = \zeta_D$ and $IS = \delta_D$, OS being parallel to the ridge line. The actual emergent ray, being along OS' , is no longer parallel to the ridge line, so that the direction of flow is changed by

the change in the shock. Its direction is more "outwards" than before, but one might expect the outwards-inwards direction of the pressure gradient to help to bring it inwards. However we are mainly considering a region where the shock deflection (the angle NAN') is small, so that S and S' are not far from one another.

From spherical trigonometry we have

$$\cos \alpha = \frac{\tan \text{IN}}{\tan \text{IA}} = \tan \zeta_D \tan \phi$$

$$\cos(\alpha - \beta) = \frac{\tan \text{IN}'}{\tan \text{IA}} = \tan \zeta \tan \phi$$

$$\cos \beta = \frac{\tan \text{IN}'}{\tan \text{IQ}} = \frac{\tan \zeta}{\tan \text{IQ}} \quad .$$

Hence we have

$$\begin{aligned} \tan \text{IQ} &= \frac{\tan \zeta}{\cos \beta} = \frac{\tan \zeta}{\cos[\alpha - (\alpha - \beta)]} \\ &= \frac{\tan \zeta}{\cos[\cos^{-1}(\tan \zeta_D \tan \phi) - \cos^{-1}(\tan \zeta \tan \phi)]} \quad , \quad (11) \end{aligned}$$

which agrees with the value (10).

Since $\tan \zeta_D$ is approximately equal to $\tan \zeta$ the denominator in (11) is close to unity and we have

$$\tan \text{IQ} \simeq \tan \zeta \quad .$$

It is not necessary for ζ itself to be small; it must not differ very much from ζ_D , which implies that the angle NAN' is small.

If in fact we write $\tan \zeta = \tan \zeta_D + \epsilon$ and ignore ϵ^3 and higher powers we find that the denominator in equation (9) may be written

$$1 - \frac{\epsilon^2 \tan^2 \phi}{1 - \tan^2 \zeta_D \tan^2 \phi} \quad .$$

We note also from Fig.7 that the maximum possible value for ζ is equal to IA , that is $90^\circ - \phi$. This was the value we used in extrapolating the pressure curves in Fig.4 to the maximum possible pressure rise across the shock.

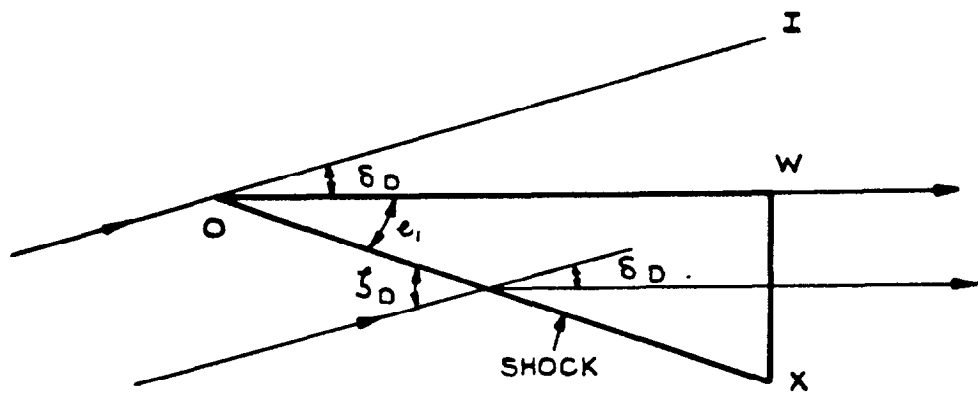
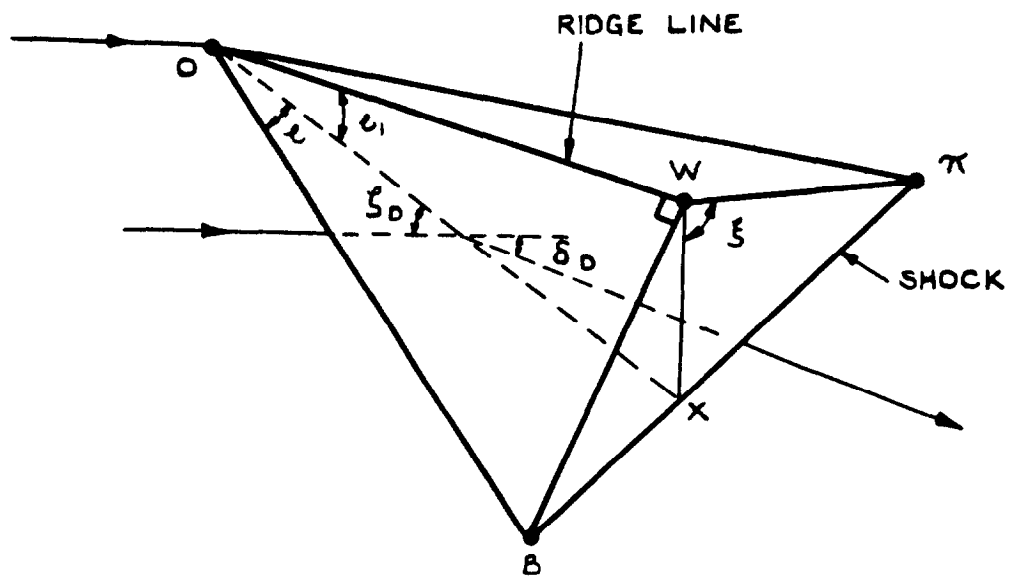


FIG.1. THE CARET SURFACE.

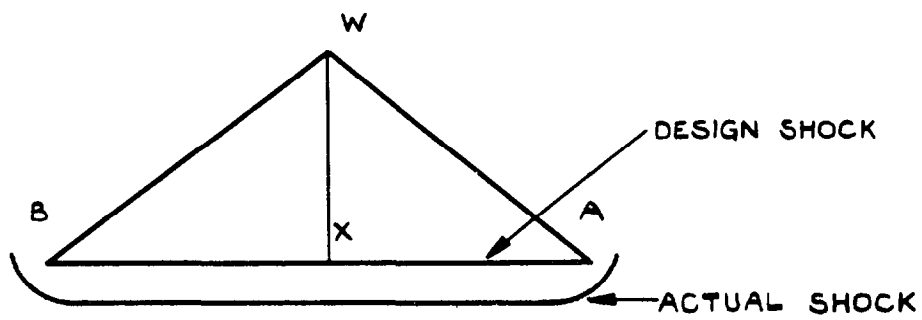
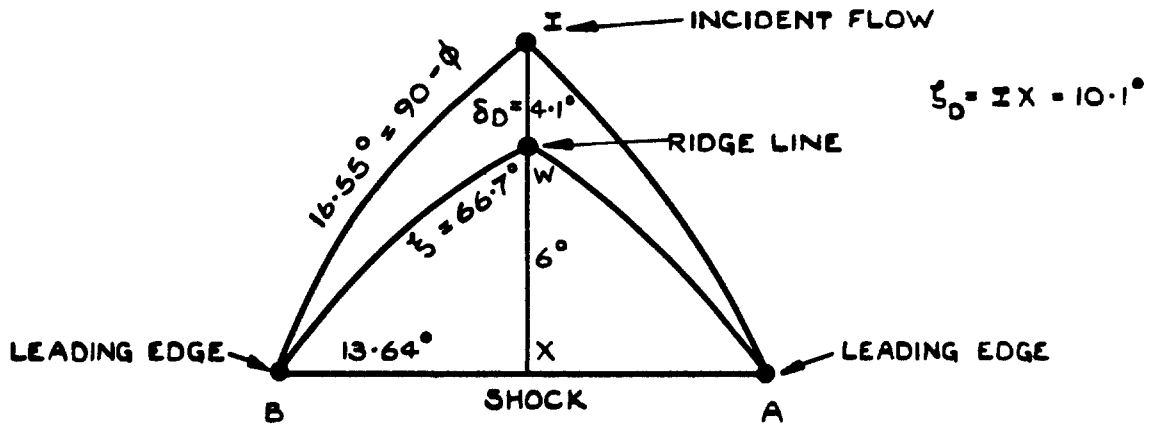
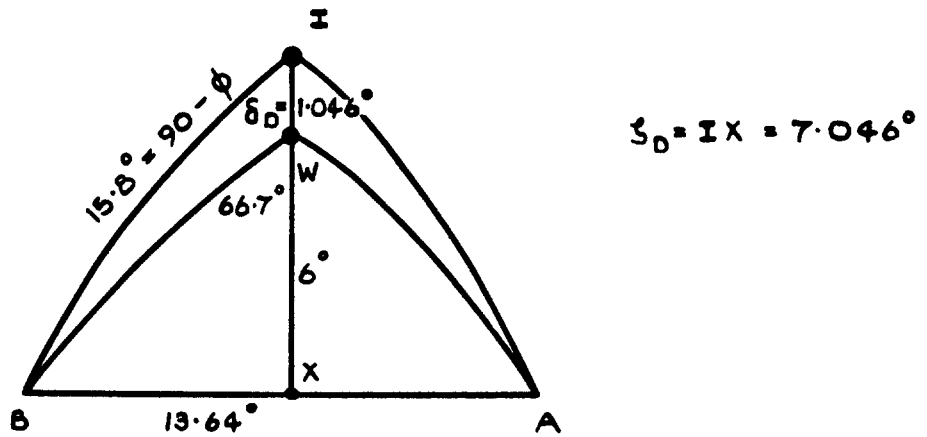


FIG. 2. PROBABLE ACTUAL SITUATION.
(STAND-OFF DISTANCE EXAGGERATED.)



CASE 1



CASE 2

FIG. 3. PROJECTION ON A SPHERE, CENTRE THE APEX.

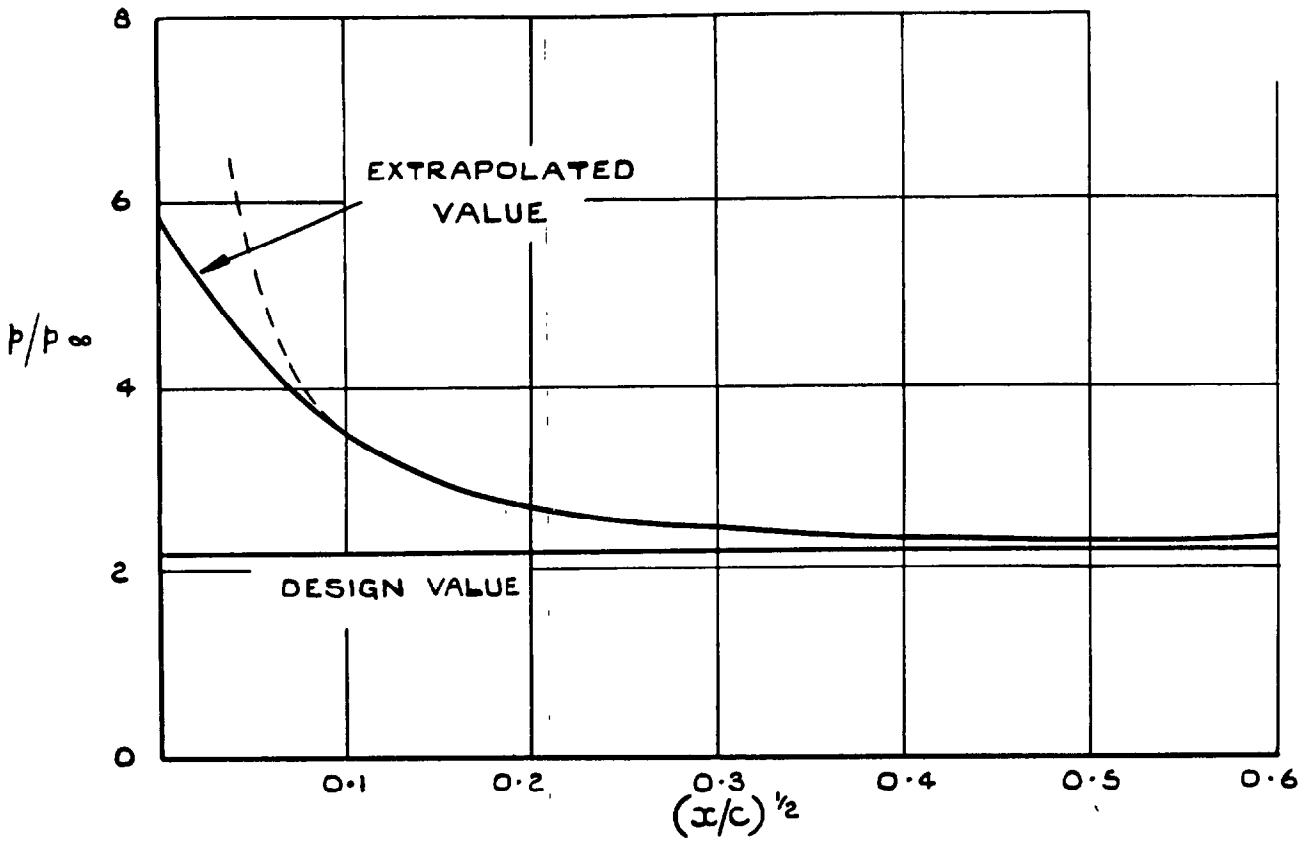


FIG.4 (a) PRESSURE RATIO. CASE 1.

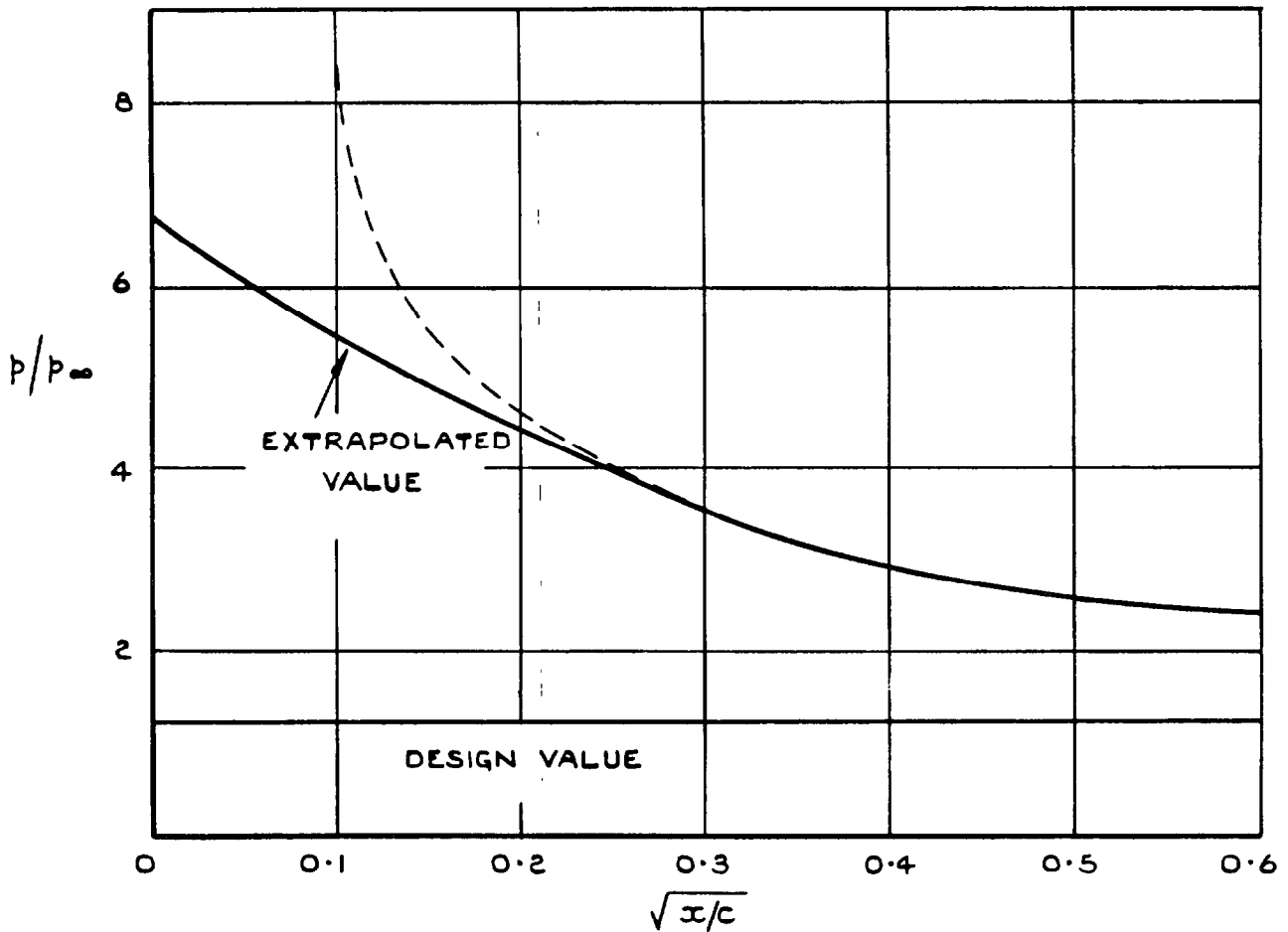


FIG.4 (b) PRESSURE RATIO. CASE 2.

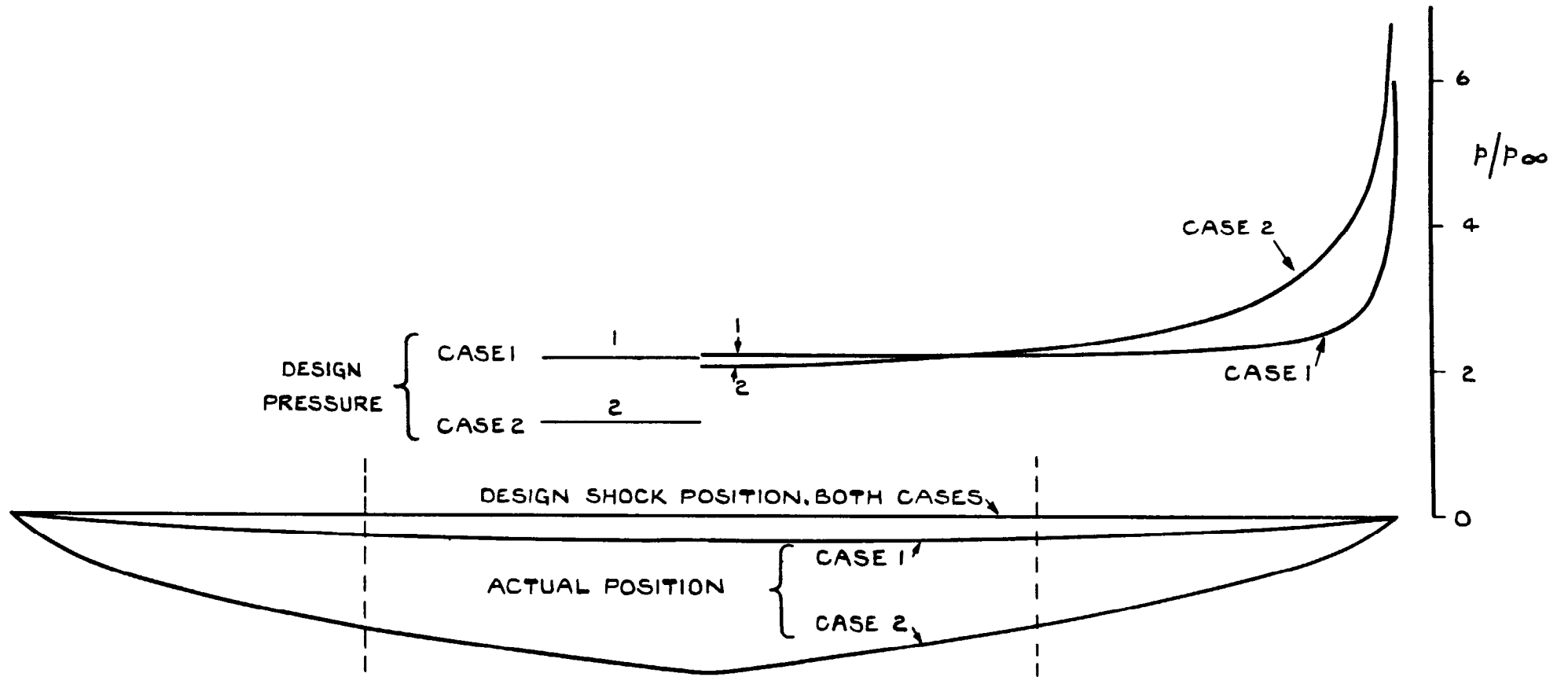


FIG.5. SHOCK POSITION AND PRESSURE DISTRIBUTION AT THE TRAILING EDGE.

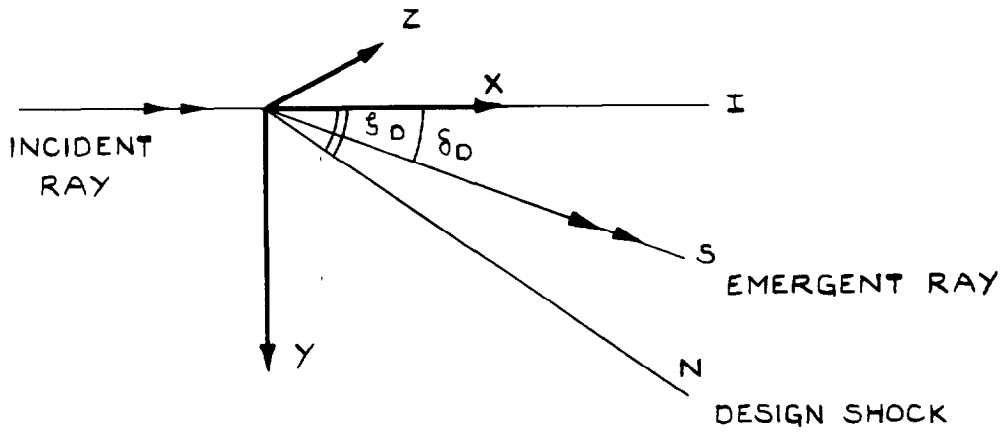


FIG. 6. CO-ORDINATE SYSTEM FOR APPENDIX I.

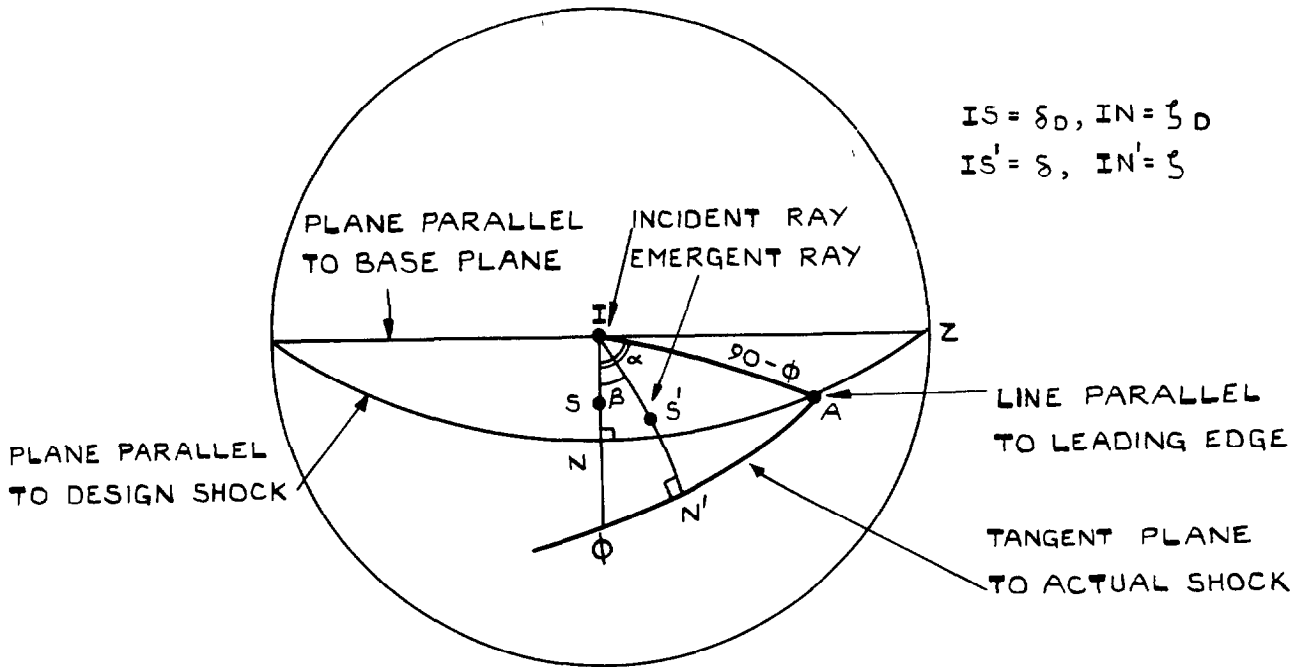


FIG. 7. PROJECTION ON A SPHERE CENTRE THE POINT O WHERE THE INCIDENT RAY MEETS THE SHOCK.

A.R.C. C.P. No.978
January 1964
J.C. Cooke

533.6.011.72 :
533.692.6

LEADING EDGE EFFECTS ON CARET WINGS

The two planes of the lower surface of a caret wing are treated as though they were infinite and swept, and the leading edge shock boundary layer interaction for each is investigated. It is found that the shock shapes are curved near to the leading edge and the pressure there is higher than the design pressure. However, in certain circumstances each shock may soon become parallel to the design shock and the pressure near to its design value. In extreme conditions this may never happen and for these cases it is concluded that the design is not achieved. A tentative condition for the achievement of design conditions is given.

A.R.C. C.P. No.978
January 1964
J.C. Cooke

533.6.011.72 :
533.692.6

LEADING EDGE EFFECTS ON CARET WINGS

The two planes of the lower surface of a caret wing are treated as though they were infinite and swept, and the leading edge shock boundary layer interaction for each is investigated. It is found that the shock shapes are curved near to the leading edge and the pressure there is higher than the design pressure. However, in certain circumstances each shock may soon become parallel to the design shock and the pressure near to its design value. In extreme conditions this may never happen and for these cases it is concluded that the design is not achieved. A tentative condition for the achievement of design conditions is given.

A.R.C. C.P. No.978
January 1964
J.C. Cooke

533.6.011.72 :
533.692.6

LEADING EDGE EFFECTS ON CARET WINGS

The two planes of the lower surface of a caret wing are treated as though they were infinite and swept, and the leading edge shock boundary layer interaction for each is investigated. It is found that the shock shapes are curved near to the leading edge and the pressure there is higher than the design pressure. However, in certain circumstances each shock may soon become parallel to the design shock and the pressure near to its design value. In extreme conditions this may never happen and for these cases it is concluded that the design is not achieved. A tentative condition for the achievement of design conditions is given.

© *Crown Copyright* 1968

Published by
HER MAJESTY'S STATIONERY OFFICE

To be purchased from
49 High Holborn, London W.C.1
423 Oxford Street, London W.1
13A Castle Street, Edinburgh 2
109 St. Mary Street, Cardiff
Brazenose Street, Manchester 2
50 Fairfax Street, Bristol 1
258-259 Broad Street, Birmingham 1
7-11 Linenhall Street, Belfast 2
or through any bookseller